



Cite this: *RSC Adv.*, 2018, 8, 6259

Received 29th November 2017
Accepted 2nd February 2018

DOI: 10.1039/c7ra12871a

rsc.li/rsc-advances

Synthesis of spiroindenopyridazine-4*H*-pyran derivatives using Cr-based catalyst complexes supported on KCC-1 in aqueous solution

Rahele Zhiani,^{ab} Seyed Mohsen Sadeghzadeh ^{*ab} and Shokufe Emrani^{ab}

An efficient bis(2-dodecylsulfanyl-ethyl)-amine·CrCl₃ complex supported on KCC-1 (KCC-1/SNS/Cr) has been developed for the synthesis of spiroindenopyridazine-4*H*-pyran, providing excellent yields of the corresponding products with remarkable chemoselectivity. This morphology ultimately leads to higher catalytic activity for the KCC-1-supported nanoparticles. The KCC-1/SNS/Cr NPs were thoroughly characterized by using TEM, SEM, TGA, FT-IR, ICP-MS, and BET. The recycled catalyst has been analyzed by ICP-MS showing only minor changes in morphology after the reaction, thus confirming the robustness of the catalyst.

Introduction

In recent years the synthesis of spiro-2-amino-4*H*-pyrans has been reported in different ways by creating variations in the three component condensation of active carbonyl compounds such as isatin, acenaphthoquinone or ninhydrin, and activated methylene reagents such as malononitrile and 1,3-dicarbonyl compounds in the presence of various catalysts leading to spiroacenaphthylenes, spirooxindoles and spiro-1,3-indanones.^{1–12}

In view of catalysis on solid supports, metal complexes with a support of choice provide a large field for the discovery of new, highly active nanocatalysts for important and challenging reactions, which also offer the additional advantage of recyclability.^{13–15} These systems have several advantages over conventional catalysts, such as superior activity and improved stability. Recently, Polshettiwar *et al.*¹⁶ reported a novel fibrous nanosilica (KCC-1) material, which has special center-radial pore structures with their pore sizes gradually increasing from the center to the surface. KCC-1 material showed a high specific surface area due to the pores in the fibers, and the accessibility of the active sites was significantly increased as a result of the special structure.^{17–21} Additionally, 3D architectures generating a hierarchical pore structure with macropores can also improve the mass transfer of the reactant.^{22,23} The KCC-1-based sorbents may have several advantages over conventional silica-based sorbents, including (i) high catalyst loading, (ii) minimum reduction in surface area after functionalization and (iii) more accessibility of the catalyst sites to

enhance the reaction, due to the fibrous structure and highly accessible surface area of KCC-1.

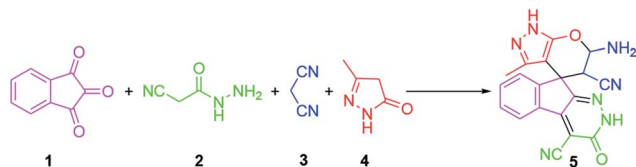
The chromium based catalysts received a great deal of attention to achieve high efficiency and selectivity toward 1-hexen production.^{24–42} Typically, these types of catalysts are Cr-complex with special ligands such as pyrrolyl,²⁴ cyclopentadienyl,^{25–28} maleimidyl^{29,30} and aryloxide^{31–33} as aromatic ligands as well as multidentate donor ligands including phosphorous, nitrogen, sulfur and oxygen atoms such as PNP,³⁴ SNS,³⁵ NNN,³⁶ NN, NO, NP and NS.^{37–42} In this regard, due to simple synthesis, readily available starting materials and low cost, the SNS ligands have been extensively explored.³⁵ On the other hand, from the viewpoint of practical applications, heterogeneous Cr-based catalysts have drawn particular attention to the simple recovery of the catalyst as well as simple purification of the product through easy filtration of solid catalyst. Although there are many literature reports for homogeneous chromium catalytic systems in the ethylene oligomerization, heterogeneous systems were rarely investigated.^{43–48} The immobilization of chromium complexes on the solid supports such as siliceous^{43–45} and polymeric supports^{46–48} are examples of heterogeneous catalysts in ethylene trimerization.

KCC-1 has been successfully utilized for various applications like CO₂ capture, photocatalysis, DNA and gene delivery, hydrogenolysis and hydro-metathesis reactions and non-carbonylative Suzuki cross-coupling reactions.^{49–60} Given our continued interest in nanocatalysis and catalyst development for organic reactions, we envisaged using bis(2-dodecylsulfanyl-ethyl)-amine·CrCl₃ complex supported on fibrous KCC-1 as a catalyst for investigate the one-pot synthesis of spiroindenopyridazine-4*H*-pyran (Scheme 1).

^aDepartment of Chemistry, Faculty of Sciences, Neyshabur Branch, Islamic Azad University, Neyshabur, Iran. E-mail: seyedmohsen.sadeghzadeh@gmail.com

^bYoung Researchers and Elite Club, Neyshabur Branch, Islamic Azad University, Neyshabur, Iran





Scheme 1 Synthesis of spiroindenopyridazine-4H-pyran in the presence of KCC-1/SNS/Cr NPs.

Experimental

Materials and methods

Chemical materials were purchased from Fluka and Merck in high purity. Melting points were determined in open capillaries using an Electrothermal 9100 apparatus and are uncorrected. FTIR spectra were recorded on a VERTEX 70 spectrometer (Bruker) in the transmission mode in spectroscopic grade KBr pellets for all the powders. The particle size and structure of nano particle was observed by using a Philips CM10 transmission electron microscope operating at 100 kV. Powder X-ray diffraction data were obtained using Bruker D8 Advance model with Cu K α radiation. The thermogravimetric analysis (TGA) was carried out on a NETZSCH STA449F3 at a heating rate of 10 °C min⁻¹ under nitrogen. ¹H and ¹³C NMR spectra were recorded on a BRUKER DRX-300 AVANCE spectrometer at 300.13 and 75.46 MHz, BRUKER DRX-400 AVANCE spectrometer at 400.22 and 100.63 MHz, respectively. Elemental analyses for C, H, and N were performed using a Heraeus CHN-O-Rapid analyzer. The purity determination of the products and reaction monitoring were accomplished by TLC on silica gel polygram SILG/UV 254 plates. Mass spectra were recorded on Shimadzu GCMS-QP5050 Mass Spectrometer.

General procedure for the preparation of KCC-1 NPs

Tetraethyl orthosilicate (TEOS) (2.5 g) was dissolved in a solution of cyclohexane (30 mL) and 1-pentanol (1.5 mL). A stirred solution of cetylpyridinium bromide (CPB 1 g) and urea (0.6 g) in water (30 mL) was then added. The resulting mixture was continually stirred for 45 min at room temperature and then placed in a Teflon-sealed hydrothermal reactor and heated 120 °C for 5 h. The silica formed was isolated by centrifugation then washed with a mixture of deionized water and acetone, and dried in a drying oven. This material was then calcined at 550 °C for 5 h in air.

General procedure for the preparation of KCC-1/3-chloropropyltriethoxysilane nanoparticles (compound 1)

2 mmol of KCC-1 NPs and 20 mL THF were mixed together in a beaker, and then 20 mmol of NaH was dispersed in to the mixture by ultrasonication. 22 mmol 3-chloropropyltriethoxysilane was added drop-wise at room temperature and stirred for another 16 h at 60 °C. The resultant products were collected and washed with ethanol and deionized water in sequence, and then dried under vacuum at 60 °C for 2 h for further use.

General procedure for the preparation of compound 2

2 mmol of KCC-1/3-chloropropyltriethoxysilane were dispersed in a mixture of 80 mL of ethanol, 20 mL of deionized water and 2.0 mL of 28 wt% concentrated ammonia aqueous solution (NH₃·H₂O), followed by the addition of 20 mmol of bis(2-chloroethyl)amine hydrochloride. After vigorous stirring for 24 h, the final suspension was repeatedly washed, filtered for several times and dried at 60 °C in the air.⁶¹

General procedure for the preparation of compound 3

25 mmol of 1-dodecanethiol was added to the 25 mmol homogenous solution of sodium hydroxide (1 g) in ethanol. Followed by, 1.5 g of compound 2 in ethanol was added to the mentioned solution and allowed to stirred for a few minutes. The solution was sequentially stirred at 0 °C for 2 h, and then 16 h at ambient temperature. The resulting liquid phase was filtrated and then ethanol was evaporated to obtain an oily liquid phase. The residue was worked up with dry normal hexane and diethyl ether. Finally, the product was obtained from the extraction of the solvent by a vacuum pump.⁶¹

General procedure for the preparation of compound 4

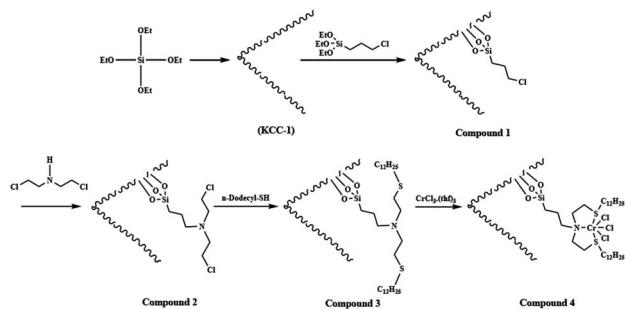
0.1 g of compound 3 was solved in tetrahydrofuran (THF). Then, 0.36 mmol of CrCl₃·(thf)₃ (0.135 g) in THF was added to reaction mixture under argon atmosphere. After 10 min, a solvent was evaporated by a vacuum pump. Then, diethyl ether was added to the product as anti-solvent and was kept overnight in a cool place. The mixture was filtered and then washed three times with diethyl ether. The green solid was obtained when the solvent was removed by vacuum. All steps in reactions were performed under argon atmosphere.⁶¹

General procedure for synthesis of spiroindenopyridazine-4H-pyran compounds

The mixture of ninhydrin **1** (1 mmol), cyanoacetohydrazide **2** (1 mmol), malononitrile **3** (1 mmol), CH-acid **4** (1 mmol), and KCC-1/SNS/Cr NPs (1 mg) in water (5 mL) was stirred at room temperature for 2 hours. Upon completion, the progress of the reaction was monitored by TLC when the reaction was completed, the catalyst was separated by filtration. Then the solvent was removed from solution under reduced pressure and the resulting residue was purified on a silica gel column (EtOAc/petroleum ether) to provide the desired ferrocene-containing quinolines.

Results and discussion

The KCC-1 core-shell was synthesized by a simple method and then functionalized by the complex of Cr, which had been obtained by the reaction between Cr and the bis-(2-dodecylsulfanyl-ethyl)-amine (SNS), according to Scheme 2. The synthesized KCC-1/SNS/Cr was then characterized by different methods such as TEM, SEM, TGA, FT-IR, and BET (Scheme 2).



Scheme 2 Schematic illustration of the synthesis for KCC-1/SNS/Cr NPs.

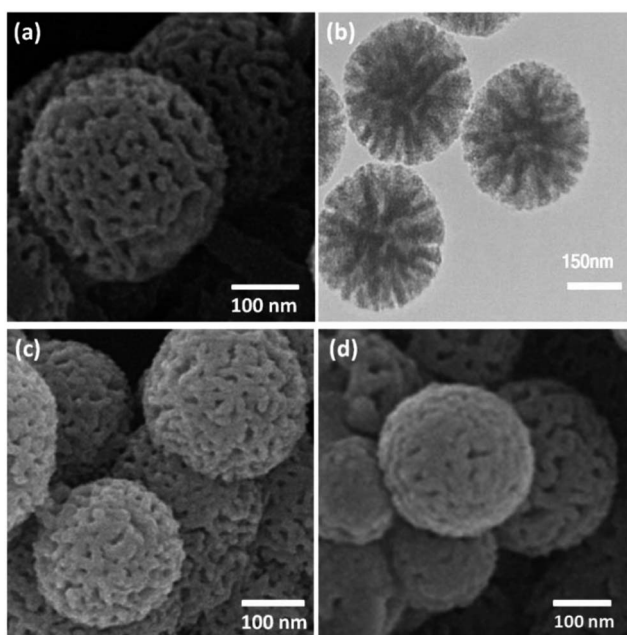


Fig. 1 SEM images of KCC-1 NPs (a); TEM images of fresh KCC-1/SNS/Cr NPs (b); SEM images of fresh KCC-1/SNS/Cr NPs (c); SEM images of KCC-1/SNS/Cr NPs after ten reuses (d).

The morphology and structure of the KCC-1 and KCC-1/SNS/Cr NPs are further characterized by SEM and TEM. Fig. 1a shows an SEM image of highly textured KCC-1 samples, where the samples have spheres of uniform size with diameters of ~ 300 nm and a wrinkled radial structure. A close inspection of these images shows that wrinkled fibers (with thicknesses of ~ 8.5 nm) grow out from the center of the spheres and are arranged radially in three dimensions. Also, the overlapping of the wrinkled radial structure forms cone-shaped open pores. The SEM image shows that the entire sphere is solid and composed of fibers. Furthermore, this open hierarchical channel structure and fibers are more easily for the mass transfer of reactants and increase the accessibility of active sites. The SEM and TEM images of KCC-1/SNS/Cr NPs showed that after modification the morphology of KCC-1 is not change (Fig. 1b and c). After being reused ten times, the dandelion-like structure of the catalyst could be still observed although the

dandelion-like structure collapsed to some extent. The structure similar between fresh KCC-1/SNS/Cr NPs and the KCC-1/SNS/Cr NPs reused ten times, accounted for high power in recyclability (Fig. 1d).

The thermal stability of the synthesized KCC-1/SNS/Cr NPs catalyst was detected through TGA and the results are depicted in Fig. 2. The weight loss below 250 °C was ascribed to the elimination of the physisorbed and chemisorbed solvent on the surface of the silica material. About 8.6% of the weight loss, in the temperature range 250 – 450 °C, was due to the organic group derivatives.

The N_2 adsorption–desorption isotherms of KCC-1/SNS/Cr NPs showed characteristic type IV curve (Fig. 3), which is consistent with literature reports on standard fibrous silica spheres. As for KCC-1, the BET surface area, total pore volume, and BJH pore diameter are obtained as 439 m^2 g^{-1} , 1.49 cm^3 g^{-1} , and 14.78 nm respectively, whereas the corresponding parameters of KCC-1/SNS/Cr NPs have decreased to 319 m^2 g^{-1} , 1.12 cm^3 g^{-1} , and 12.21 nm. The nitrogen sorption analysis of KCC-1/SNS/Cr NPs also confirms a regular and uniform mesostructure with a decrease in surface area, pore diameter and pore volume parameters in comparison with that of pristine KCC-1. With the functionalization by bis-(2-dodecylsulfanyl-ethyl)-amine-Si, the corresponding pore volumes are drastically reduced. This could be ascribed to increased loading with the sensing probe, which occupies a large volume inside the silica spheres (Fig. 3 and Table 1).

FT-IR spectroscopy was employed to determine the surface modification of the synthesized catalyst (Fig. 4). The Si–O–Si symmetric and asymmetric stretching vibrations at 802 cm^{-1} and 1103 cm^{-1} and the O–H stretching vibration at 3444 cm^{-1} were observed for the KCC-1 (Fig. 4a). The O–H stretching vibration at 3439 cm^{-1} , the Si–O stretching at 1108 cm^{-1} , the CH_2 stretching at 2910 cm^{-1} were observed for the KCC-1/SNS/Cr NPs (Fig. 4b). These results indicated that the organic compound had been successfully introduced onto the surface of KCC-1.

To optimize reaction conditions for the KCC-1/SNS/Cr NPs catalyst system, the effects of various reaction parameters were investigated. We examined the effect of solvent on the synthesis of spiroindenopyridazine-4*H*-pyran using the KCC-1/SNS/Cr

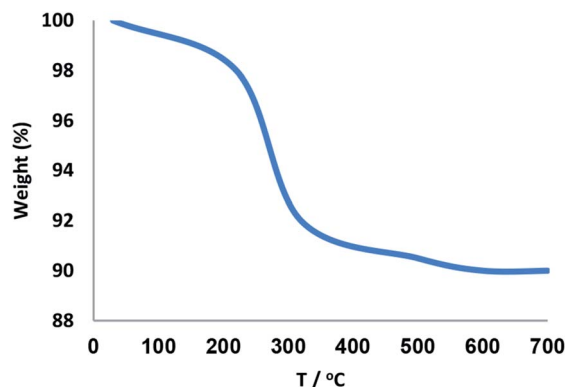


Fig. 2 TGA diagram of KCC-1/SNS/Cr NPs.

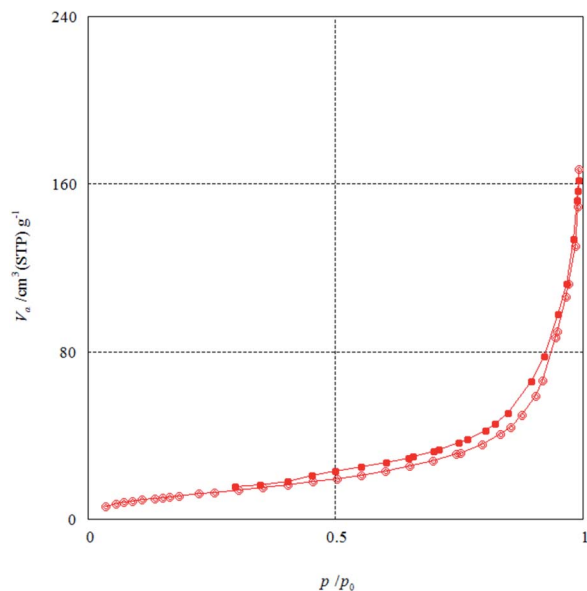


Fig. 3 Adsorption–desorption isotherms of KCC-1/SNS/Cr.

Table 1 Structural parameters of KCC-1 and KCC-1/SNS/Cr NPs materials determined from nitrogen sorption experiments

Catalysts	S_{BET} ($\text{m}^2 \text{g}^{-1}$)	V_a ($\text{cm}^3 \text{g}^{-1}$)	D_{BJH} (nm)
KCC-1	439	1.49	14.78
KCC-1/SNS/Cr NPs	319	1.12	12.21

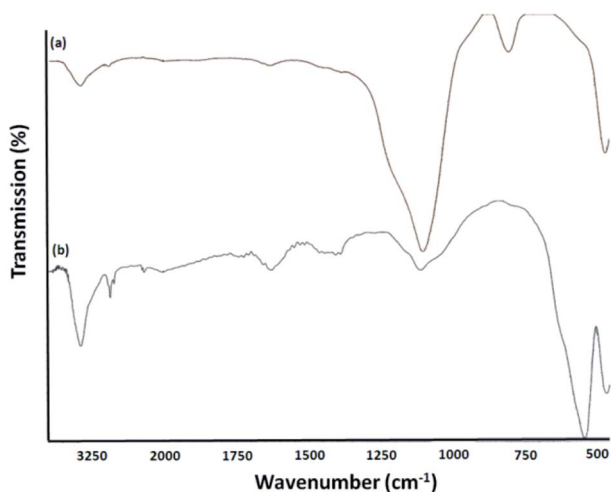


Fig. 4 FTIR spectra of (a) KCC-1, (b) KCC-1/SNS/Cr NPs.

NPs at heating under reflux (Table 2). Solvent does affect on catalysts performance. *n*-Hexane, benzene, CCl_4 , or cyclohexane, a non-polar solvent, gave spiroindenopyridazine-4*H*-pyran a lower yield (Table 2, entry 12–15). CH_3CN , THF, CH_2Cl_2 , DMF, toluene, dioxane, CHCl_3 , EtOAc, and DMSO, aprotic polar solvents, gave also spiroindenopyridazine-4*H*-pyran in low yields. The reaction was do better in protic solvent. *i*-PrOH, and

Table 2 The effect of solvent and temperature for synthesis of spiroindenopyridazine-4*H*-pyran^a

Entry	Solvent	Temp. ($^{\circ}\text{C}$)	Yield ^b (%)
1	EtOH	Reflux	64
2	H_2O	Reflux	96
3	H_2O	80	96
4	H_2O	60	96
5	H_2O	r.t.	96
6	CH_3CN	r.t.	36
7	THF	r.t.	25
8	CH_2Cl_2	r.t.	29
9	EtOAc	r.t.	43
10	DMF	r.t.	24
11	Toluene	r.t.	27
12	<i>n</i> -Hexane	r.t.	18
13	Benzene	r.t.	9
14	CCl_4	r.t.	17
15	Cyclohexane	r.t.	12
16	CHCl_3	r.t.	43
17	DMSO	r.t.	32
18	MeOH	r.t.	72
19	Dioxane	r.t.	24
20	<i>i</i> -PrOH	r.t.	55
21	Solvent-free	r.t.	—

^a Reaction conditions: ninhydrin **1** (1 mmol), cyanoacetohydrazide **2** (1 mmol), malononitrile **3** (1 mmol), dimedone **4** (1 mmol), solvent (10 mL), and catalyst (1 mg), 2 h. ^b GC yields [%].

ethanol gave spiroindenopyridazine-4*H*-pyran in average yields (Table 2, entries 1 and 20). In contrast, the use of methanol resulted in an increased yield of 72% the yield was remarkably increased up to 96% when H_2O was used as the solvent respectively in the presence of KCC-1/SNS/Cr NPs. In this study, it was found that water is a more efficient (Table 2, entry 2) over other organic solvents. A solvent that stabilizes one of two competing transition states that control the selectivity should enhance the selectivity of the product obtained *via* the stabilized transition state. For example, in multicomponent reactions higher reaction rates and selectivities are often obtained in polar solvents compared to non-polar solvents, which has been attributed to enhanced hydrogen bonding between the solvent and the transition state, as well as to enforced hydrophobic interactions when conducted in water, which facilitates alignment of the substrates. The ability to use water as the reaction medium greatly increases the green credentials of the method. We also investigated the crucial role of temperature in the synthesis of spiroindenopyridazine-4*H*-pyran in the presence of KCC-1/SNS/Cr NP as a catalyst. Results clearly indicated that the catalytic activity isn't sensitive to reaction temperature. The best temperature for this reaction was at room temperature (Table 2, entry 2–5).

As shown in Fig. 5, the amount of catalyst also has a significant effect on the coupling reaction. The reaction rate was accelerated quickly in the range 0.6–0.8 mg. However, the yield decreased when the amount of catalyst reached 2.0 mg. Based on these report, it can be inferred that increasing amount of catalyst was propitious to produce spiroindenopyridazine-4*H*-pyran when the amount of catalyst was less than 1.8 mg.

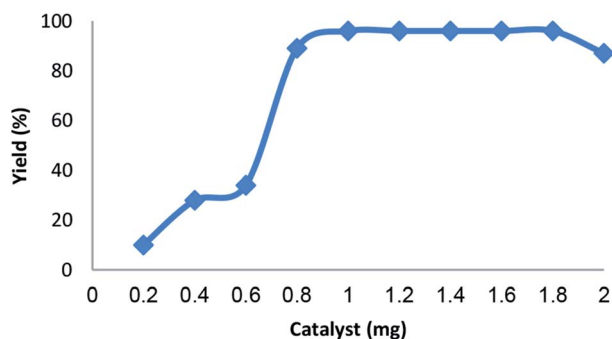


Fig. 5 Effect amount of catalyst on yield of spiroindenopyridazine-4H-pyran.

Therefore, the amount of catalyst of 1.0 mg was considered as suitable condition.

The influence of time on this reaction is exhibited in Fig. 6. It is obvious that the spiroindenopyridazine-4H-pyran yield increased up to 96% for 120 min. Whereas further increase in the time don't resulted in a slight decrease in the product yield. Therefore, the optimal time for the coupling reaction of ninhydrin, cyanoacetohydrazide, malononitrile, and dimedone are 120 min.

For further investigation the efficiency of the catalyst, different control experiments were performed and the obtained information is shown in Table 3. Initially, a standard reaction was carried out using KCC-1 showed that any amount of the desired product was not formed after 2 h of reaction time (Table 3, entries 1). Also, when KCC-1/SNS was used as the catalyst, a reaction was not observed (Table 3, entries 2). The bis-(2-dodecylsulfanyl-ethyl)-amine could not give the satisfactory catalytic activity under mild reactions. Based on these disappointing results, we continued the studies to improve the yield of the product by added the Cr. Notably, there was not much difference in the reaction yields when reaction was carried out using KCC-1/SNS/Cr NPs and $\text{CrCl}_3 \cdot (\text{thf})_3$ catalyst (Table 3, entries 3 and 7), however, $\text{CrCl}_3 \cdot (\text{thf})_3$ is not recoverable and reusable for the next runs. These observations show that the reaction cycle is mainly catalyzed by Cr species complexed on the KCC-1/SNS nanostructure. The nano-sized particles increase

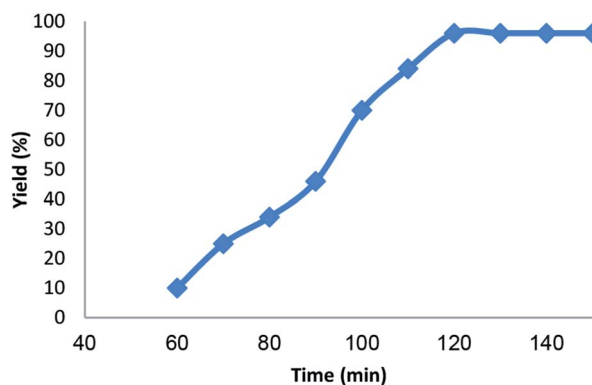


Fig. 6 Effect of time on yield of spiroindenopyridazine-4H-pyran.

Table 3 Influence of different catalysts for synthesis of spiroindenopyridazine-4H-pyran^a

Entry	Catalyst	TOF ^b (h ⁻¹)
1	KCC-1	—
2	KCC-1/SNS	—
3	KCC-1/SNS/Cr	48
4	Nano-SiO ₂ /SNS/Cr	21.5
5	MCM-41/SNS/Cr	42.5
6	SBA-15/SNS/Cr	43.5
7	$\text{CrCl}_3 \cdot (\text{thf})_3$	47.5

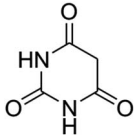
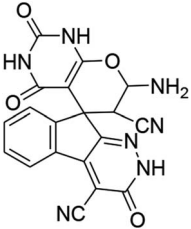
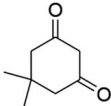
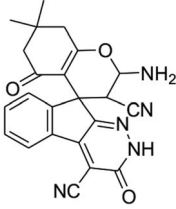
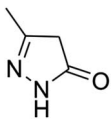
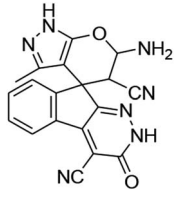
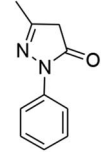
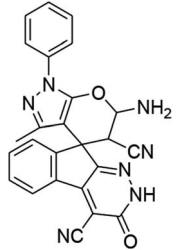
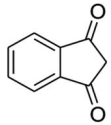
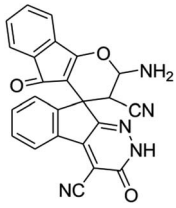
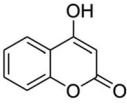
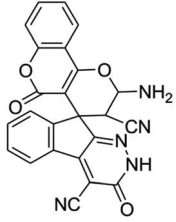
^a Reaction conditions: ninhydrin **1** (1 mmol), cyanoacetohydrazide **2** (1 mmol), malononitrile **3** (1 mmol), and dimedone **4** (1 mmol), 2 h.
^b Isolated yield.

the exposed surface area of the active site of the catalyst, thereby enhancing the contact between reactants and catalyst dramatically and mimicking the homogeneous catalysts. As a result, KCC-1/SNS/Cr NPs was used in the subsequent investigations because of its high reactivity, high selectivity and easy separation. Also, the activity and selectivity of nano-catalyst can be manipulated by tailoring chemical and physical properties like size, shape, composition and morphology. To assess the exact impact of the presence of KCC-1 in the catalyst, the KCC-1/SNS/Cr NPs compared with MCM-41/SNS/Cr, SBA-15/SNS/Cr, and nano-SiO₂/SNS/Cr. When nano-SiO₂/SNS/Cr, MCM-41/SNS/Cr or SBA-15/SNS/Cr was used as the catalyst, the yield of the desired product was average to good, but the yield for KCC-1/SNS/Cr was excellent. Non-negligible activity of the silica was attributed to its shape, composition and morphology. Besides, the large space between fibers can significantly increase the accessibility of the active sites of the KCC-1. That is why, the KCC-1 was more effective than nano-SiO₂, MCM-41, and SBA-15 (Table 3, entries 3–6). As a result, KCC-1 NPs were used in the subsequent investigations because of its high reactivity, high selectivity and easy separation (Table 3).

To examine the scope of the catalytic properties of the catalyst for synthesis of spiroindenopyridazine-4H-pyran, various types of CH-acids **4** were reacted with ninhydrin **1**, cyanoacetohydrazide **2** and malononitrile **3** in the presence of a catalytic amount of KCC-1/SNS/Cr NPs. It was found that all these CH-acids **4** were suitable for this reaction, giving the desired products excellent yields (Table 4).

The loading amount of Cr in Nano-SiO₂/SNS/Cr, MCM-41/SNS/Cr, SBA-15/SNS/Cr, and KCC-1/SNS/Cr NPs as determined by ICP-MS. The amount of Cr in nano-SiO₂/SNS/Cr, MCM-41/SNS/Cr, SBA-15/SNS/Cr, and KCC-1/SNS/Cr were 1.4, 2.1, 2.3, and 2.9 wt%, respectively. The higher metal loading obtained for KCC-1/SNS/Cr can be attributed to the larger initial surface area of KCC-1 when compared with nano-SiO₂, MCM-41 and SBA-15. Also, Cr leaching was studied by inductively coupled plasma mass spectrometry (ICP-MS) analysis of the catalyst, after ten cycles of reactions. The loading amount of Cr after ten reuses was found to be 2.8 wt%, which shows negligible Cr leaching (Table 5, entry 8). The amount of Cr in nano-SiO₂/SNS/Cr, MCM-41/SNS/Cr, and SBA-15/SNS/Cr were 0.8, 1.7, and 1.8 wt%, which shows Cr leaching (Table 5, entries 5–7). This

Table 4 Synthesis of spiroindenopyridazine-4*H*-pyran derivatives in the presence of KCC-1/SNS/Cr NPs^a

Entry	CH-acid	Product	Yield ^b (%)	mp (°C)
1			95	>300 (ref. 62)
2			96	>300 (ref. 62)
3			96	293–296 (ref. 62)
4			98	270–272 (ref. 62)
5			93	>300 (ref. 62)
6			92	>300 (ref. 62)

^a Reaction conditions: ninhydrin 1 (1 mmol), cyanoacetylhydrazide 2 (1 mmol), malononitrile 3 (1 mmol), CH-acids 4 (1 mmol), and catalyst (1 mg), 2 h. ^b GC yields [%].

remarkable ability of the KCC-1/SNS/Cr mesostructure may be attributed to fibres of KCC-1 that effectively manage the reaction through preventing Cr agglomeration and releasing and recapturing Cr during reaction process.

It is important to note that the heterogeneous property of KCC-1/SNS/Cr NPs facilitates its efficient recovery from the reaction mixture during work-up procedure. The activity of the recycled catalyst was also examined under the optimized

Table 5 The loading amount of Cr

Entry	Catalyst	wt%
1	Nano-SiO ₂ /SNS/Cr	1.4
2	MCM-41/SNS/Cr	2.1
3	SBA-15/SNS/Cr	2.3
4	KCC-1/SNS/Cr	2.9
5	Nano-SiO ₂ /SNS/Cr after ten reuses	0.8
6	MCM-41/SNS/Cr after ten reuses	1.7
7	SBA-15/SNS/Cr after ten reuses	1.8
8	KCC-1/SNS/Cr after ten reuses	2.8

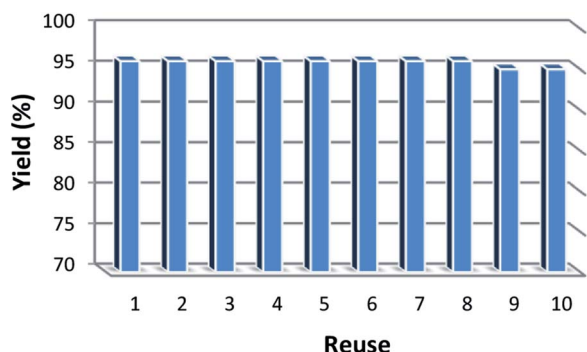


Fig. 7 The reusability of catalysts for synthesis of spiroindenopyridazine-4H-pyran.

conditions. After the completion of reaction, the catalyst was separated by filtration, washed with methanol and dried at the pump. The recovered catalyst was reused for ten consecutive cycles without any significant loss in catalytic activity (Fig. 7). This lack of reduction in catalyst performance can be attributed to the simple and stability of the catalyst structure.

Conclusions

In the present study KCC-1/SNS/Cr NPs was synthesized and characterized as an environmentally-friendly nanocatalyst for the synthesis of spiroindenopyridazine-4H-pyran with various CH-acids substrates. The experimental results displayed the core-shell structure of the synthesized catalyst with a mean size range of 250–300 nm. In addition, the catalyst was easily recoverable and reusable. Subsequently, high yields in short reaction times were achieved without the need for an expensive Cr catalyst as well as excellent reusability for at least ten times in the corresponding reaction without a reduction in catalytic activity.

Conflicts of interest

There are no conflicts to declare.

Notes and references

1 P. Saluja, K. Aggarwal and J. M. Khurana, *Synth. Commun.*, 2013, **43**, 3239–3246.

- 2 R. Baharfar and R. Azimi, *Synth. Commun.*, 2014, **44**, 89–100.
- 3 G. Mohammadi Ziarani, M. Hosseini, N. Lashgari, A. Badiei, M. Amanlou and R. Bazl, *J. Nanostruct.*, 2013, **2**, 489–500.
- 4 H. R. Safaei, M. Shekouhy, S. Rahmanpur and A. Shirinfeshan, *Green Chem.*, 2012, **14**, 1696–1704.
- 5 M. N. Elinson, A. I. Ilovaisky, V. M. Merkulova and P. A. Belyakov, *Tetrahedron*, 2012, **68**, 5833–5837.
- 6 A. Hasaninejad, A. N. Golzar, M. Beyrati, A. Zare and M. M. Doroodmand, *J. Mol. Catal. A: Chem.*, 2013, **372**, 137–150.
- 7 J. Zheng and Y. Li, *Mendeleev Commun.*, 2012, **22**, 148–149.
- 8 F. Macaev, N. Sucman, F. Shepeli, M. Zveaghintseva and V. Pogrebnoi, *Symmetry*, 2011, **3**, 165–170.
- 9 B. Sadeghi, F. Baharestan, A. Kafi and A. Hassanabadi, *Bulg. Chem. Commun.*, 2016, **49**, 331–334.
- 10 L. Jalili-Baleh, N. Mohammadi, M. Khoobi, L. Mamani, A. Foroumadi and A. Shafiee, *Helv. Chim. Acta*, 2013, **96**, 1601–1609.
- 11 B. Karmakar, A. Nayak and J. Banerji, *Tetrahedron Lett.*, 2010, **53**, 5004–5007.
- 12 R. Ghahremanzadeh, G. Hosseini, R. Akbarzadeh and A. Bazgir, *J. Heterocycl. Chem.*, 2013, **50**, 272–280.
- 13 V. Polshettiwar and T. Asefa, *Nanocatalysis: Synthesis and Applications*, 2013.
- 14 V. Polshettiwar, *Angew. Chem., Int. Ed.*, 2013, **52**, 11199.
- 15 P. Serp and K. Philippot, *Nanomaterials in Catalysis*, Wiley-VCH, Weinheim, 2013, p. 496.
- 16 V. Polshettiwar, D. Cha, X. Zhang and J. M. Basset, *Angew. Chem.*, 2010, **49**, 9652–9656.
- 17 V. Polshettiwar, J. Thivolle-Cazat, M. Taoufik, F. Stoffelbach, S. Norsic and J. M. Basset, *Angew. Chem.*, 2011, **50**, 2747–2751.
- 18 U. Patil, A. Fihri, A.-H. Emwas and V. Polshettiwar, *Chem. Sci.*, 2012, **3**, 2224.
- 19 A. Fihri, D. Cha, M. Bouhrara, N. Almana and V. Polshettiwar, *ChemSusChem*, 2012, **5**, 85–89.
- 20 A. Fihri, M. Bouhrara, U. Patil, D. Cha, Y. Saih and V. Polshettiwar, *ACS Catal.*, 2012, **2**, 1425–1431.
- 21 A. S. Lilly Thankamony, C. Lion, F. Pourpoint, B. Singh, A. J. Perez Linde, D. Carnevale, G. Bodenhausen, H. Vezin, O. Lafon and V. Polshettiwar, *Angew. Chem.*, 2015, **54**, 2190–2193.
- 22 N. D. Petkovich and A. Stein, *Chem. Soc. Rev.*, 2013, **42**, 3721–3739.
- 23 C. M. Parlett, K. Wilson and A. F. Lee, *Chem. Soc. Rev.*, 2013, **42**, 3876–3893.
- 24 W. K. Reagan, EP 0417477, Phillips Petroleum Company, 1991.
- 25 G. J. P. Britovsek, V. C. Gibson and D. F. Wass, *Angew. Chem., Int. Ed.*, 1999, **38**, 428–447.
- 26 K. H. Theopold, *Eur. J. Inorg. Chem.*, 1998, 15–24.
- 27 R. Emrich, O. Heinemann, P. W. Jolly, C. Kruger and G. P. J. Verhovnik, *Organometallics*, 1997, **16**, 1511–1513.
- 28 H. Mahomed, A. Bollmann, J. Dixon, V. Gokul, L. Griesel, C. Grove, F. Hess, H. Maumela and L. Pepler, *Appl. Catal.*, A, 2003, **255**, 355.

- 29 T. Aoyama, H. Mimura, T. Yamamoto, M. Oguri and Y. Koie, JP 9176299(A), Tosoh Corporation, 1991.
- 30 H. Mimura, T. Aoyama, T. Yamamoto, M. Oguri and Y. Koie, JP 09268133, Tosoh Corporation, 1997.
- 31 D. C. Commereuc, R. M. Drochon and C. Saussine, *US Pat.*, 6031145, Institut Francais du Petrole, 1998.
- 32 D. C. Commereuc, R. M. Drochon and C. Saussine, EP 1110930, Institut Francais du Petrole, 2001.
- 33 D. H. Morgan, S. L. Schwikkard, J. T. Dixon, J. J. Nair and R. Hunter, *Adv. Synth. Catal.*, 2003, **345**, 939–942.
- 34 D. S. McGuinness, P. Wasserscheid, W. Keim, C. Hu, U. Englert, J. T. Dixon and C. Grove, *Chem. Commun.*, 2003, 334.
- 35 D. S. McGuinness, P. Wasserscheid, W. Keim, D. H. Morgan, J. T. Dixon, A. Bollmann, H. Maumela, F. Hess and U. Englert, *J. Am. Chem. Soc.*, 2003, **125**, 5272–5273.
- 36 M. E. Bluhm, O. Walter and M. Doring, *J. Organomet. Chem.*, 2005, **690**, 713–721.
- 37 L. J. Ackerman, X. Bei, T. R. Boussie, G. M. Diamond, K. A. Hall, A. M. Lapointe, J. M. Longmire, V. J. Murphy, P. Sun, D. Verdugo, S. Schofer, E. Dias, D. H. McConville, R. T. Li, J. Walzer, F. Rix and M. Kuchta, WO2006096881, Exxon-Mobil, 2006.
- 38 D. H. McConville, L. J. Ackerman, R. T. Li, X. Bei, M. Kuchta, T. R. Boussie, J. F. Walzer, G. M. Diamond, F. C. Rix, K. A. Hall, A. M. La Pointe, J. M. Longmire, V. J. Murphy, P. Sun, D. V. Verdugo, S. Schofer and E. Dias, WO2006099053, Exxon-Mobil, 2006.
- 39 L. J. Ackerman, G. M. Diamond, K. A. Hall, J. M. Longmire, V. J. Murphy and D. Verdugo, WO2008085659, Exxon-Mobil, 2008.
- 40 L. J. Ackerman, G. M. Diamond, K. A. Hall, J. M. Longmire, V. J. Murphy and V. O. Nava-Salgado, WO2008085653, Exxon-Mobil, 2008.
- 41 L. J. Ackerman, G. M. Diamond, K. A. Hall, J. M. Longmire and M. Micklatcher, WO2008085655, Exxon-Mobil, 2008.
- 42 L. J. Ackerman, G. M. Diamond, K. A. Hall, J. M. Longmire, V. J. Murphy and D. Verdugo, WO2008085658, Exxon-Mobil, 2008.
- 43 H. Monoi and Y. Sasaki, *J. Mol. Catal. A: Chem.*, 2002, **187**, 135–141.
- 44 C. N. Nenu and B. M. Weckhuysen, *Chem. Commun.*, 2005, 1865–1867.
- 45 C. N. Nenu, J. N. J. van Lingen, F. M. F. de Groot, D. C. Koningsberger and B. M. Weckhuysen, *Chem.-Eur. J.*, 2006, **12**, 4756.
- 46 N. Peulecke, B. H. Mller, S. Peitz, B. R. Aluri, U. Rosenthal, A. Wehl, W. Mller, M. H. Al azmi and M. F. Mosa, *ChemCatChem*, 2010, **2**, 1079.
- 47 S. Liu, Y. Zhang, Y. Han, G. Feng, F. Gao, H. Wang and P. Qiu, *Organometallics*, 2017, **36**, 632–638.
- 48 M. L. Shoji and H. B. Friedrich, *S. Afr. J. Chem.*, 2012, **65**, 214–222.
- 49 A. Fihri, M. Bouhrara, D. Cha and V. Polshettiwar, *ChemSusChem*, 2012, **5**, 85–89.
- 50 M. Dhiman and V. Polshettiwar, *J. Mater. Chem. A*, 2016, **4**, 12416–12424.
- 51 V. Polshettiwar, J. Thivolle-Cazat, M. Taoufik, F. Stoffelbach, S. Norsic and J. M. Basset, *Angew. Chem., Int. Ed.*, 2011, **50**, 2747–2751.
- 52 M. Bouhrara, C. Ranga, A. Fihri, R. R. Shaikh, P. Sarawade, A.-H. Emwas, M. N. Hedhili and V. Polshettiwar, *ACS Sustainable Chem. Eng.*, 2013, **1**, 1192–1199.
- 53 A. S. L. Thankamony, C. Lion, F. Pourpoint, B. Singh, A. J. P. Linde, D. Carnevale, G. Bodenhausen, H. Vezin, O. Lafon and V. Polshettiwar, *Angew. Chem., Int. Ed.*, 2015, **54**, 2190–2193.
- 54 U. Patil, A. Fihri, A. H. Emwas and V. Polshettiwar, *Chem. Sci.*, 2012, **3**, 2224–2229.
- 55 B. Singh and V. Polshettiwar, *J. Mater. Chem. A*, 2016, **4**, 7005–7019.
- 56 R. Singh, R. Bapat, L. Qin, H. Feng and V. Polshettiwar, *ACS Catal.*, 2016, **6**, 2770–2784.
- 57 X. Huang, Z. Tao, J. C. Praskavich Jr, A. Goswami, J. F. Al-Sharab, T. Minko, V. Polshettiwar and T. Asefa, *Langmuir*, 2014, **30**, 10886–10898.
- 58 Z. S. Qureshi, P. B. Sarawade, I. Hussain, H. Zhu, H. Al-Johani, D. H. Anjum, M. N. Hedhili, N. Maity, V. Delia and J. M. Basset, *ChemCatChem*, 2016, **8**, 1671–1678.
- 59 S. M. Sadeghzadeh, *Catal. Commun.*, 2016, **72**, 91–96.
- 60 S. M. Sadeghzadeh, *Catal. Sci. Technol.*, 2016, **6**, 1435–1441.
- 61 Z. Mohamadnia, E. Ahmadi, M. Nekoomanesh Haghighi and H. Salehi-Mobarakeh, *Catal. Lett.*, 2011, **141**, 474–480.
- 62 M. Bayat and H. Hosseini, *New J. Chem.*, 2017, **41**, 14954–14959.